A hybrid mechanistic-empirical approach to the modelling of twin screw feeders for continuous tablet manufacturing

Davide Bascone,[*,†] Federico Galvanin,[‡] Nilay Shah,[†] and Salvador Garcia-Munoz[¶]

†*Centre for Process System Engineering, Department of Chemical Engineering, Imperial College London, London, SW7 2AZ, United Kingdom*

‡*Centre for Process System Engineering, Department of Chemical Engineering, University College London (UCL), London, WC1E 6BT, United Kingdom*

¶*Eli Lilly and Company, Lilly Research Laboratories, Indianapolis, Indiana, IN 46285, United States*

E-mail: d.bascone@imperial.ac.uk

Abstract

Nowadays, screw feeders are popular equipment in the pharmaceutical industry. However, despite the increasing research in the last decade in the manufacturing of powder-based products, there is still a lack of knowledge on the physics governing the dynamic behaviour of these systems. As a result, data-driven models have often been used to address process design, optimisation and control applications.

In this paper, a methodology for the modelling of twin screw feeders has been suggested. A first order plus dead time model has been developed where a hybrid mechanistic-empirical approach has been used. Different powders and two screw feeder geometries have been investigated. The model predictions are in good agreement with the experimental measurements when the 35-mm diameter screws are employed. When the 20 mm- diameter screws are used, the validity range of the model is limited for the least cohesive powders, suggesting that their screw speed-dependant resistance to flow in small screws requires further investigations.

Keywords

Dynamic modelling, Screw feeders, Continuous tablet manufacturing, Pharmaceutical

1 Introduction

Over the last decade, the potential application and advantages of the continuous manufacturing of powder-based processes in the pharmaceutical industry have been widely investigated[1–14]. This research interest is consistent with the Quality-by-Design (QbD) initiative promoted by the U.S. Food and Drug Administration (FDA), which essentially aims to enhance the process understanding and encourage the development of methodologies for online measurements of material properties, real-time control, optimisation and design space[2,5,6].

In continuous tablet manufacturing feed rate accuracy is essential, in order to ensure the required ratios between different ingredients (API, lubricant and excipient) for the desired formulation[6,15]. However, cohesive and poorly flowing powders can be difficult to accurately feed. Screw feeders are commonly employed for powder metering in continuous tablet manufacturing. They consist of a hopper, as receptacle of the powder, a flow-aid system, which is typically an agitator, and one or two ("twin") screws which act as a conveying mechanism. The mass flow rate is controlled by continuously weighing the feeder and adjusting the screw speed. These feeders are also called "loss-in-weight feeder". They operate under "gravimetric mode" when the control system regulates the screw speed to correct the mass flow rate (closed loop system), whilst they run under "volumetric mode" during refill operations (open loop system), as the weight of the feeder is increasing[7].

Notwithstanding the increasing research in particle technologies and pharmaceutical applications, the development of first-principles models of feeders is limited[16] and the behaviour of bulk solids is still being investigated[9]. They may exhibit both solid- and liquid- like behaviour and it is not well understood how physical properties and operating and geometrical variables interact and affect the feeding operation[17,18]. Thus, the problem is often treated like a black-box process. Data-driven modelling techniques, such as response surface or kriging techniques, have been proposed by several authors to predict the feeder behaviour[1,18].

A large number of physical properties of the bulk solid may significantly affect the feeder performance. Examples of important material properties are cohesion, particulate descriptors, compressibility, rheology, flow, permeability and porosity[19]. Multivariate methods have been suggested to develop predictive models for both volumetric and gravimetric modes[5,20]. A statistical approach was also suggested by Engish and Muzzio to predict the performance of loss-in-weight feeders[6]. They developed a methodology for characterisation of feeders, using relative standard deviation and analysis of variance (ANOVA) to describe the effect of feeder tooling, powder and screw speed on the feeder performance.

Empirical or semi-empirical models have been proposed to predict the mass flow rate out of a feeder in closed loop systems. Boukouvala et al.[2] proposed a first order delay differential equation to predict the mass flow rate out of a feeder:

$$\tau \frac{d\dot{m}(t)}{dt} + \dot{m}(t) = kN \tag{1}$$

$$\Theta \frac{\partial \dot{m}_{actual}(t,z)}{\partial t} = -\frac{\partial \dot{m}_{actual}(t,z)}{\partial t} \tag{2}$$

with initial condition $\dot{m}_{actual}(t, z = 0) = \dot{m}(t)$. In Eqs. 1–2, $\dot{m}(t)$ is the time-dependant mass flow rate, $\dot{m}_{actual}(t, z)$ refers to the actual mass flow rate (delayed) out of the feeder, N refers to the screw speed, z is the delay domain, τ, k and Θ are model parameters.

A semi-empirical approach was suggested by Escotet-Espinoza et al.[4,21]. These authors considered the effects of the pressure exerted by the powder in the hopper on the feed factor *ff*, defined as the amount of solids within one screw pitch volume, according to the following equations:

$$ff(t) = ff_{sat} - \exp[\beta m(t)](ff_{sat} - ff_{min}) \tag{3}$$

where m is the mass of bulk solids in the hopper, β, ff_{sat} and ff_{min} are parameters regressed from data. Then, the resulting mass flow rate was estimated as:

$$\dot{m}(t) = ff(t)N(t) \tag{4}$$

Yu and Arnold[22] and Roberts[23] suggested physics-based models to estimate the average, time-independent powder feed rate. These authors suggested theoretical expressions to estimate the volumetric efficiency η_v due to vortex motion of the particulates. Then, the product between η_v and the degree of fill or "fullness" of the screws η_f provides the overall volumetric efficiency η, which is defined as the ratio between the volume of particulates conveyed and the screw volume available during one revolution. Once that the volumetric efficiency is known, assuming constant bulk density ρ_b, the average time-independent mass flow rate can be calculated as:

$$\dot{m} = \rho_b \eta N V_{ScrewPitch} \tag{5}$$

Discrete Element Method (DEM) simulations have also been widely used to gain a better understanding of the particulate behaviour in the feeding operations[24–30]. These methods can accurately predict particle packing, mass flow and mixing[10]. However, their complexity requires high computational efforts and a proper calibration of the physical properties of the particles to mimic the real system.

In this manuscript, a mathematical model to predict the dynamic mass flow rate out of twin screw feeders is presented. The vertical stress distribution in the hopper is estimated for different hopper geometries, applying the so-called "slice element method"[31–34]. The vertical stress is assumed to determine the effective powder density within the twin screws, using an empirical relationship suggested in the literature[31,35]. Geometrical details of the twin screws are used to calculate the volume flow rate. The volumetric efficiency due to the vortex motion of the particulates is also considered in the calculations, as it may significantly affect the feed rate. The mathematical model can be applied to different powders and screw feeder geometries. The range of model applicability in terms of screw speed depends on the powder properties and screw geometries.

The remainder of the paper is organised as follows. Section 2 provides details of feeders and bulk solids used in the experimental investigations. In section 3 the mathematical model is presented. The model calibration and testing against experimental data, under volumetric mode, are discussed in section 4. Finally, the paper concludes with a general discussion of the model and its future developments in section 5.

2 Experimental set-up and materials

Experimental mass flow rates, kindly provided by Eli Lilly and Company, have been used to develop and test the mathematical model. A total of 16 experiments involving different powders, feeders and operating conditions were carried out. Below, feeders and bulk solids are described.

2.1 Screw feeders

The experimental data were obtained using two different feeders, Coperion K-Tron KT20 and Coperion K-Tron KT35 (the numbers 20 and 35 indicate the size of the screw flight, expressed in mm). Further geometrical details of the two twin screw feeders are not disclosed due to confidentiality reasons. The feeders have, at the bottom of the hopper, a small bowl (volume of a few litres) with an agitator as flow-aid system. A sketch of the equipment is shown in Figure 1.

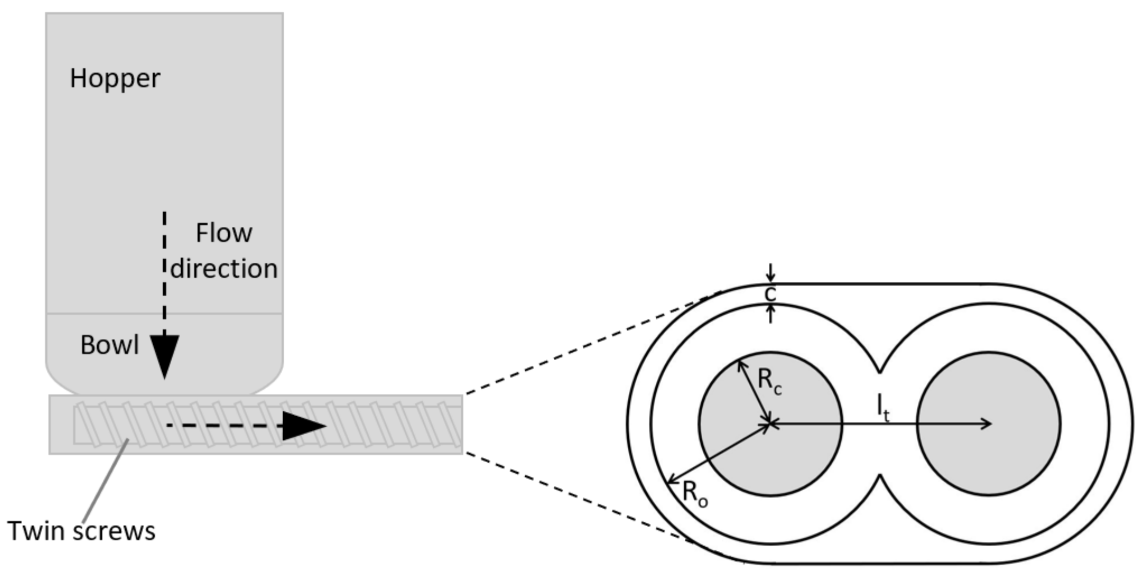

Figure 1: Sketches of the screw feeder (left, side view) and the cross sectional area of the twin screws (right, enlarged). In the latter, casing and screws are shown. The grey areas, i.e. the cross sectional area of the core shafts, do not contribute to the cross sectional area available.

2.2 Powders

Six different solids have been investigated: mannitol SD-100, lactose monohydrate, microcrystalline cellulose Avicel PH 101 and 102, crosscarmellose sodium and sodium stearyl fumarate. Some physical properties of the aforementioned materials, experimentally achieved or taken from the literature[36–40], are listed in Table 1 in the supporting information available at http://pubs.acs.org. Although the number of bulk solids investigated is limited, their characteristics are diverse and equally distributed in terms of cohesiveness and flowability: according to the classification based on the Hausner ratio[41,42], mannitol and lactose are non-cohesive, microcrystalline cellulose PH 101 and sodium stearyl fumarate are cohesive and microcrystalline cellulose PH 102 and crosscarmellose sodium are in the transitional group. Wall friction angles and effective angles of internal friction of crosscarmellose sodium and sodium stearyl fumarate have been roughly estimated assuming linearity with respect to the flow function coefficients, due to the lack of data. These approximated estimations are justified by the limited impact of these two physical properties on the model predictions (refer to the supporting information provided for further details on sensitivity analyses).

3 Mathematical modelling

The mathematical model of twin screw feeders, suitable for continuous tablet manufacturing, is presented in this section. Physics-based models suggested in the literature have been used to predict volumetric efficiency in the screws and to determine the stress distribution along the hopper length. The vertical stress is assumed to affect the effective powder density within the screws, which is considered a time-dependant variable. The delayed dynamic of the feeder is also considered. Below, a detailed description of the model is given.

3.1 Time-dependant mass flow rate

To develop the predictive model of twin screw feeders, the following assumptions have been made:

- the adhesion of the powder to the surface of screws and casing is supposed to be neglected as "self-cleaning" twin concave, used in the experimental data, are expected to minimise this phenomenon (this is an assumption, not an observation from experimental investigations);
- phenomena which may cause irregular hopper discharges, such as ratholing and arching behaviour[43], have been neglected: experimental torque measurements did not show them, probably because of the presence of a flow-aid system (agitator) which spins at a few rpm to gently breaks up cohesive materials;
- The risk of funnel flow is neglected and the vertical stress along the hopper's height is estimated according to this assumption. The extent of funnel flow is reduced by the presence of the agitator. Any further effect of the agitator in the bowl, which represents a small portion of the overall hopper volume (approximately from 20% to 10%, depending of the equipment used), has been neglected at this stage.

A First Order Plus Dead Time (FOPDT) model, known to adequately describe the dynamics of several industrial application[44,45], has been used to satisfactorily describe the mass flow rates out of a feeder according to the following equations:

$$\tau \frac{d\dot{m}(t)}{dt} + \dot{m}(t) = \dot{m}_{level}(t) \tag{6}$$

$$\dot{m}_{actual}(t) = \dot{m}(t - \theta) \tag{7}$$

where τ is the time constant, $\dot{m}_{actual}(t)$ is the actual, delayed, mass flow rate, θ is the dead time. The mass flow rate $\dot{m}_{level}(t)$ is the mass flow rate reached after the initial delayed first order response, i.e. approximately after $4\tau+\theta$[46]. The noise in the mass flow rate is neglected. The mass flow rate is calculated via a physics-based approach considering the screw geometry and the effective powder density $\rho_{eff}(t)$:

$$\dot{m}_{level}(t) = nPAN\rho_{eff}(t)\eta \tag{8}$$

where n is the number of starts of the screw thread, P is the screw pitch, A is the cross sectional area calculated as follows:

$$A = 2\pi(R_o^2 - R_c^2) + \pi(2cR_o + c^2) + 2cl_t + 2R_ol_t - \pi R_o^2 \tag{9}$$

The meaning of the geometrical parameters R_o, R_c, c and l_t are depicted in Figure 1.

3.2 Theoretical volumetric efficiency

The following equations have been included in the mathematical model to predict the volumetric efficiency η_v due to vortex motion of the particulates:

$$\eta_v = \frac{\tan\beta}{\tan\alpha + \tan\beta} \tag{10}$$

$$\beta = \tan^{-1}\left[\frac{\pi(R_o + R_c) - \mu P}{P + \pi\mu(R_o + R_c)}\right] \tag{11}$$

$$\alpha = 90^\circ - \phi - \beta \tag{12}$$

where μ is the friction coefficient[16,22] and ϕ is the wall friction angle. Equations 10–12 were suggested by Yu and Arnold[16], who derived those relationships from the analyses of the particulate mechanics. Depending on the friction coefficient μ, η_v can range between approximately 0.7 and 1, proportionally affecting the volume flow rate deliverable and, consequently, the mass flow rate. For an extensive description of the vortex motion of the particulates, the reader is referred to[16,22]. The overall volumetric efficiency η is calculated as the product between η_v and the degree of fill η_f. In this work, the degree of fill is incorporated in the effective density ρ_{eff}, as previously suggested by other authors[4,21]. The calculation of the effective density will be described in the next section.

The friction coefficient μ has to be estimated to predict the volumetric efficiency. Yu reported very close predictions of η_v when using Eq. 10 and the following equation[23]:

$$\eta_v = 1 - \frac{1 + 2\pi\mu\zeta_{av}}{4\pi^2\zeta_{av}^2 + 1} \tag{13}$$

where $\zeta_{av} = (\zeta_o + \zeta_c)/2$, with $\zeta_o = R_o/P$ and $\zeta_c = R_c/P$.

Therefore, to reduce the number of model parameters, μ has been calculated as first approximation assuming Eq. 10 = Eq. 13 and solving for μ. The friction coefficients used in this work are listed in Table 2 in the supporting information.

3.3 Time-dependant powder density

As suggested by Escotet-Espinoza et al.[21] and confirmed experimentally, for a constant screw speed the mass flow rate decreases as the hopper fill level decreases. The amount of solids in the hopper exerts a vertical stress on the powder entering the twin screws, which affects how the powder fills the available volume between the surface of the screws and the casing.

Several empirical relationships have been suggested in the literature to correlate stress and density of food and pharmaceutical powders[47–51]. However, here the effective powder density incorporates the degree of fill of the screws, as previously mentioned. Hence, the effective powder density differs from the bulk density. The effective density has been satisfactorily predicted by the empirical relationship suggested by Malave *et al.*, which can be reformulated as follows[31,35]:

$$\rho_{eff}(t) = \rho_0 + \kappa \ln\left[\frac{\sigma_v(t)}{1000}\right] \tag{14}$$

where ρ_0 describes the effective density under no vertical stress, σ_v is the vertical stress expressed in kPa. Both ρ_0 and κ are found by fitting the model to experimental data.

The estimation of the effective density by the vertical stress allows to explore the impact of the hopper geometry and friction properties on the feed rate.

3.4 Vertical stress distribution in the hopper

The stress distribution along the height of the hopper, for symmetrical geometry, can be estimated from the equilibrium of forces. The stress distribution depends on both hopper geometry and powder properties. It also depends on the state of stress, which can be active (during the filling of the hopper, also called "static condition") or passive (during the discharging, also called "dynamic condition")[31,34]. In the static condition, the lines of major principal stresses are predominantly vertical. In the dynamic condition, because of flowing solids, the lines of the major principal stresses are predominantly horizontal[33,52,53]. However, only a portion of the particle bed in the hopper is affected by the dynamic condition. It can be assumed that the upper section of the hopper is undisturbed by the withdrawal of the powder. Therefore, during the emptying phase, the stress distribution in the upper section is still in a static condition. Hence, there is a point of discontinuity at the transition between the stress distribution in dynamic condition, with horizontal major principal stress (at the bottom of the hopper), and the stress distribution still in static condition, with vertical major principal stress (at the top section of the hopper). This point of discontinuity is known as "switch point" and has been investigated by several authors[33,52,53]. In the case of a cylindrical hopper with conical bottom end and assuming that all particles are in motion during the emptying (i.e. no funnel flow), the location of the switch point is typically assumed at the transition from vertical walls to inclined walls[43,53], as shown in Figure 2.

The switch point, in this work, is assumed between the hopper and the bowl at the bottom, where the flow-aid system is installed and the geometry changes. Further experimental and computational investigations may be beneficial to validate this assumption. However, when performing a sensitivity analysis, according to the model the location of the switch point is not crucial for the predicted mass flow rate (see supporting information).

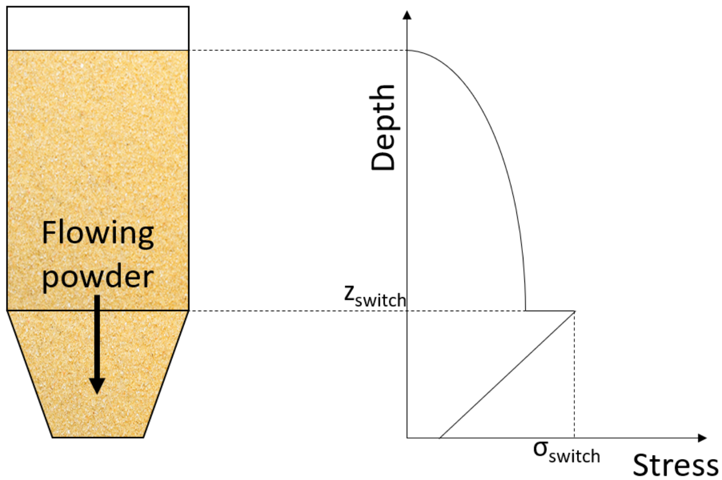

Figure 2: Example of vertical stress distribution in a hopper, assuming the switch point at the transition from vertical to inclined walls. The stress distribution depends on the powder properties.

3.4.1 Cylindrical hopper

From the equilibrium of vertical forces in an infinitesimal element (Figure 3), using the so-called "slice element method", with cylindrical hopper and assuming constant bulk density in the hopper, the following non-homogeneous differential equation can be obtained:

$$A\sigma_v + g\rho_b A dz = A(\sigma_v + d\sigma_v) + \tau_w U dz \tag{15}$$

Integrating Equation 15 and assuming $\sigma_v = 0$ at z=0, *i.e.* free surface at the top of the hopper, the dimensionless average vertical stress $\bar{S}_z = \bar{\sigma_v}/\rho_b g d$ (d is the hopper diameter) in static conditions can be calculated as follows[52]:

$$\bar{S}_{z,s} = \frac{1}{4B_s D_s}(1 - e^{-4B_s D_s Z}) \tag{16}$$

where B_s and D_s are function of both effective angle of internal friction and angle of friction at the wall, Z is the dimensionless depth z/d. The subscript s refers to the static condition.

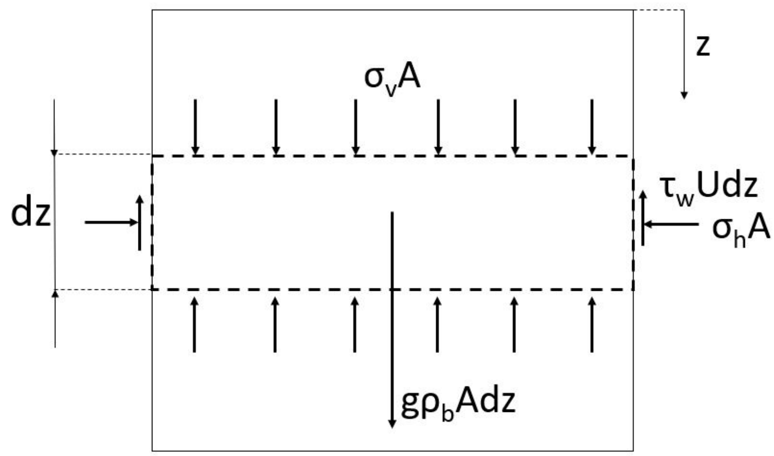

Figure 3: Forces acting on a slice element in an infinitesimal section of a cylindrical hopper. The sides of the slides are assumed to be parallel to the hopper walls. A is the cross sectional area, U the perimeter, all the other symbols have their usual meaning.

Below the switch point, the dimensionless average vertical stress $\bar{S}_z$ is computed from:

$$\bar{S}_{z,d} = \frac{1}{4B_d D_d}[1 - e^{-4B_d D_d (Z - Z_{sw})}] + \bar{S}_{z_{sw}} e^{-4B_d D_d (Z - Z_{sw})} \quad (17)$$

where $\bar{S}_{z_{sw}}$ is the dimensionless average vertical stress calculated at the switch point, which occurs at depth z_{sw} and is calculated by Eq. 16. The subscript d refers to the dynamic condition. The reader is referred to[52] for the detailed derivation of the dimensionless stress in cylindrical hoppers, such as the one used with the feeder K-Tron KT20. For other geometries, such as conical or wedge-shaped hoppers, Equations 16–17 are not valid, as the equilibrium of forces slightly differs[32,33,43,54,55].

3.4.2 Conical hopper

An asymmetrical conical hopper was used with the feeder K-Tron KT35. The asymmetrical geometry leads to three linear ordinary differential equations to simultaneously be solved to predict the stress distribution. Limited studies are available for the rigorous estimation of stress distribution in asymmetrical hoppers[56].

It is assumed in this work that, for conical hoppers, the vertical stress is mainly affected by the height of powder and that the asymmetrical cone can be approximated by a symmetrical one.

The equilibrium of vertical forces in an infinitesimal element of a symmetrical conical hopper is given by[33]:

$$\frac{d\bar{\sigma}}{dz} + \frac{4\bar{\sigma}}{d - 2z\tan\alpha}[ED + \tan\alpha(D-1)] = \rho_b g \tag{18}$$

where E is function of wall friction angle[33], effective angle of internal friction and wall inclination α. From integration of Eq. 18, at static condition and assuming free surface at the top of the hopper, the dimensionless average vertical stress $\bar{S}_z$ is[33]:

$$\bar{S}_{z,s} = \frac{1 - 2Z\tan\alpha}{2\tan\alpha(K_s - 1)}[1 - (1 - 2Z\tan\alpha)^{K_s - 1}] \tag{19}$$

where $K_s = 2(E_s D_s/\tan\alpha + D - 1)$.

When emptying, in dynamic conditions, $\bar{S}_z$ is calculated as follows:

$$\bar{S}_{z,d} = \frac{1 - 2Z\tan\alpha}{2\tan\alpha(K_d - 1)}\left[1 - \left(\frac{1 - 2Z\tan\alpha}{1 - 2Z_{sw}\tan\alpha}\right)^{K_d - 1}\right] + \bar{S}_{z_{sw}}\left(\frac{1 - 2Z\tan\alpha}{1 - 2Z_{sw}\tan\alpha}\right)^{K_d} \tag{20}$$

where $\bar{S}_{z_{sw}}$ is calculated with Eq. 19 at $Z = Z_{sw}$. Due to the limited impact on the results (Figure 12), at this stage the switch point has been assumed between hopper and bowl, similarly to the cylindrical hopper.

3.5 Time-dependant hopper fill level

At each instant t, the dimensionless vertical stress exerted on the bottom of the hopper is estimated by Eq. 17 when using cylindrical hoppers, whilst by Eq. 20 when using conical hoppers. The depth z is the hopper fill level $H(t)$. The latter depends on the time-dependant particle bed volume $V(t)$ in the feeder hopper (intended as the whole receptacle, bowl included) and its mass $m(t)$:

$$H(t) = f(V(t)) \tag{21}$$

$$V(t) = m(t)/\rho_b \tag{22}$$

$$\frac{d(m(t) - m_{in})}{dt} = -\dot{m}_{actual}(t) \tag{23}$$

where $f(V(t))$ is a generic function of the particle bed volume in the hopper and depends on the hopper geometry, either conical or cylindrical. In the latter, the height is simply the ratio between the particle bed volume and the cross sectional area of the hopper. In the conical hopper, the fill level is correlated to the weight of powder through a second order polynomial regression. m_{in} is the mass of solids initially loaded into the hopper. The mass of solids in the twin screws can be neglected.

As can be noted from the mass balance in the feeder hopper (Eq. 23), no periodic refill has been considered at this stage.

4 Model performance

The experimental behaviour of six of the most commonly used powders in the pharmaceutical industry has been studied. All powders were investigated at two different screw speeds using the feeder K-Tron KT20. Additionally, two powders were also investigated using the feeder K-Tron KT35, at two screw speeds. Further information on the experimental settings are given in the supporting information. The goal is to identify a general model that can capture the dynamics of several powders in different conditions.

4.1 Model calibration

The mathematical model consists of Eqs.6–12, 14, 21–23 and either Eqs. 16–17 (when cylindrical hopper is used with K-Tron KT20) or Eqs. 19–20 (when conical hopper with

K-Tron KT35). Four model parameters are required:

1. τ, the time constant in Eq. 6, which describes the step response of the mass flow rate;

2. θ, *i.e.* the dead time in Eq. 7;

3. ρ_0, which is the effective powder density within the screws assuming no vertical stress, see Eq. 14;

4. κ, which relates the vertical stress and the effective powder density according to Eq. 14.

The mathematical model has been posed as an unconstrained optimisation model and the four parameters above have been identified by minimising the mean square error MSE between experimental and predicted values:

$$\text{MSE} = \frac{1}{n}\sum_{i=1}^{n}(\dot{m}_{exp} - \dot{m}_{predicted})^2 \tag{24}$$

Below, a description of data and procedure used for the model calibration is given.

4.1.1 Experimental data

A total of sixteen experiments, twelve using K-Tron KT20 and four using K-Tron KT35, have been investigated. Eight experiments have been used to calibrate the model, one for each powder and feeder, whilst the remaining eight have been used to test the model. The feeder was run under volumetric mode. Except when using microcrystalline cellulose Avicel PH 102 in the K-Tron KT20 at 7.71 rpm, all experiments were carried out until no more powders were fed out of the screw feeder. In general, the weight of the residual material in the hopper was lower than 200 g. The experimental mass flow rates were calculated as $\dot{m}_{exp} = \Delta m_{exp}/\Delta t$ at each point. The sampling rate is not constant but automatically determined by the equipment. To smooth the data and simplify the parameter estimation, a thirty-point centred moving average was calculated. The experimental data set have been further cleaned removing initial negative flow rates (which cannot be calculated by the model), when present, and peaks significantly larger than the average mass flow rate (over one order of magnitude). For most of the bulk solids, an abrupt drop in the mass flow rate occurs after the feed rate becomes lower than the average feed rate by approximately 30%. This indicates that the hopper is almost empty. Below this minimum hopper fill level, the mass flow rate quickly approaches zero and a limited number of experimental points were obtained. These values have a negligible effect on the model parameters and have not been considered when calculating the mean squared error.

4.1.2 Solution procedure

The model parameters have been identified using two solvers for unconstrained optimisations in MATLAB, *fminsearch* and *fminunc*. No significant differences have been observed using both solvers. Ordinary differential equations have been solved using the solver *ode45*, based on an explicit Runge-Kutta (4,5) formula. For a few of experiments, involving a large number of data points and higher fluctuations in the mass flow rate, the solver *ode45* have not provided good fits. For these data, lower-order but more robust solvers such as *ode23* or *ode23s* have been used instead.

4.1.3 Estimated parameters

The model calibration is discussed in this section. The identified parameters are listed in Table 1.

The calculated mass flow rate using lactose monohydrate and microcrystalline cellulose Avicel PH 102 with K-Tron KT20 and K-Tron KT35 are shown respectively in Figure 4, Figure 5 and Figure 6. The calibrated model captures well the trend of the mass flow rates, despite the significantly differences in the feeder geometries, operating conditions and powder properties. The largest deviation from the experimental data has been achieved using lactose monohydrate in K-Tron KT20 at 77.1 rpm (Figure 4). In this case, the system dynamics is not accurately described by a first order differential equation, as both the initial increase and then the decrease of the feed rate are almost linear with time. However, the first order response remains the most suitable trend to generally describe the mass flow rates experimentally investigated here. Boukouvala et al.[2] suggested a first order differential model as well, despite they included a system delay.

Table 1: Parameter estimation results. Acronyms used for bulk solids: MCC=Microcrystalline Cellulose Avicel PH, CCS=Crosscarmellose Sodium, SSF=Sodium Stearyl Fumarate.

Bulk solid	Speed [rpm]	ρ_0 [kg m^{-3}]	κ [kg m^{-3}]	τ [s]	θ [s]	MSE	Feeder
Mannitol	7.71	253.27	23.93	99.77	54.35	3.20×10^{-3}	K-Tron KT20
Mannitol	19.2	552.52	2.79	14.57	5.81	$9.60\ \times10^{-3}$	K-Tron KT35
Lactose	77.1	561.15	50.82	14.78	0.00	5.09×10^{-1}	K-Tron KT20
MCC 101	38.50	86.22	1.26	14.22	33.43	2.10×10^{-3}	K-Tron KT20
MCC 102	7.71	187.12	-63.31	13.52	92.51	1.60×10^{-3}	K-Tron KT20
MCC 102	38.4	354.00	12.68	11.46	4.50	1.52×10^{-1}	K-Tron KT35
CCS	61.70	314.31	26.38	12.98	27.70	6.51×10^{-2}	K-Tron KT20
SSF	61.70	131.23	10.46	17.98	8.20	2.40×10^{-3}	K-Tron KT20

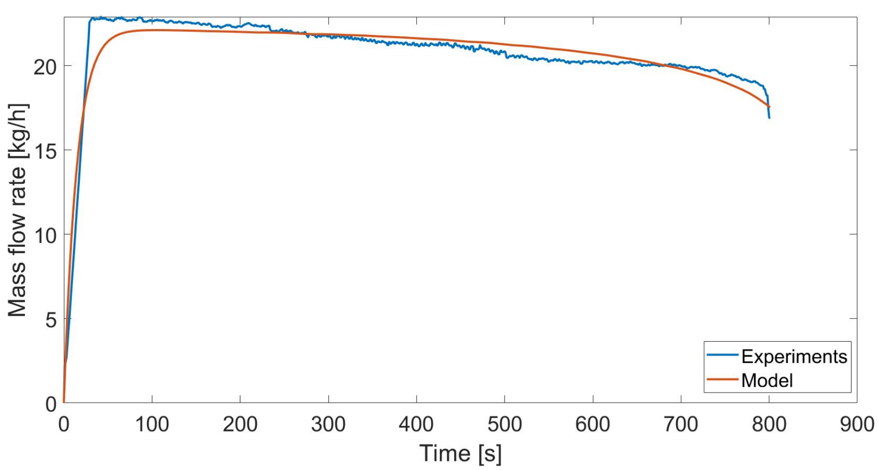

Figure 4: Model calibration using lactose monohydrate, feeder K-Tron KT20, screw speed 77.1 rpm. The blue line represents the measured values, the red line is the model response.

The physical properties of the materials, the feeder geometry and the operating conditions

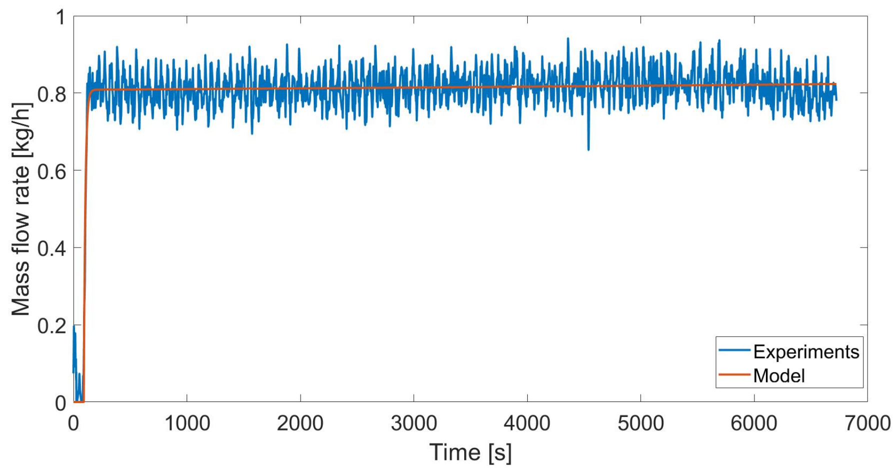

Figure 5: Model calibration using microcrystalline cellulose PH 102, feeder K-Tron KT20, screw speed 7.71 rpm. The blue line represents the measured values, the red line is the model response.

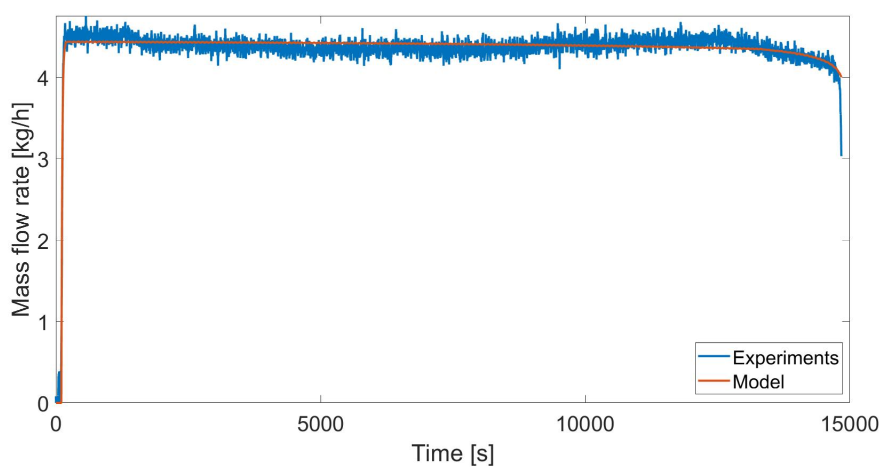

Figure 6: Model calibration using microcrystalline cellulose PH 102, feeder K-Tron KT35, screw speed 6.4 rpm. The blue line represents the measured values, the red line is the model response.

significantly affect the withdrawal of the powder from the hopper outlet and their conveyance through the screws. Hence, different dead times are achieved. Generally, the dead time decreases as the screw speed increases, according to the decreased residence time of the bulk solids within the twin screws. However, when using lactose monohydrate, the estimated dead time θ is zero (see Table 1), which is not consistent with the geometry of the equipment. This is due to the experimental investigations in question. In fact, in the said three cases, to overcome the initial reluctance of the powder in the hopper to flow downwards, the motor had been turned on and off before the actual experimental feeding operation, at constant screw speed and until the hopper is emptied (no interruptions), started. Therefore, when the actual experiment started, the screws were already partially filled by the materials and the powder in the hopper had already been in motion, in contrast to the other experiments where the operation started with unfilled screws. As a result, a mass flow rate was immediately recorded when the motor was turned on. These data may be used only to partially describe the system dynamics during the start up.

In Table 2, estimated dead times and mean residence times along the screws (in the choke section, i.e. in the section of the screws extending beyond the hopper exit, and including the estimated degree of fill) are shown. In most of the investigated cases, the dead time is larger than the residence time, which may indicate also some resistance for the powder to be discharged from the hopper from a static condition. Using mannitol with feeder K-Tron KT35, the dead times is shorter than the residence time probably because of some solid residuals on the screws before the start of the experiment (before it was run at 19.4 rpm, it had been run for approximately 10 s at 12.7 rpm).

The values in Table 2 suggest that the overall delay is a function of physical properties and operating conditions. The short number of experimental data used does not allow for the identification of the nature of the dead time over different configurations, which is the objective of future works. The mean residence time, calculated as the ratio between holdup and feed rate, can be used as dead time only as a rough estimation. Furthermore, the calculated dead time will be relevant only for the description of start up operations. If this is the case, the residence time may be used as a good estimation of θ when refilling. Further experimental investigations, including refill, are required to gain a better understanding of the main causes of the dead time in different conditions. At this stage, the values of θ from the model calibrations are more accurate to predict the start-up only if the screw speed is not markedly varied from the values used in the model calibration, otherwise the residence time can be a reasonable estimate.

Table 2: Comparison between estimated dead time θ and mean residence time along the screws.

Bulk solid	Feeder	Speed [rpm]	θ [s]	Mean residence time [s]
Mannitol	K-Tron KT20	7.71	54.35	34.85
Mannitol	K-Tron KT35	19.20	5.81	16.49
Lactose	K-Tron KT20	77.10	0.00	3.42
MCC 101	K-Tron KT20	38.50	33.43	6.64
MCC 102	K-Tron KT20	7.71	92.51	32.94
MCC 102	K-Tron KT35	38.40	4.50	8.25
CCS	K-Tron KT20	61.70	27.70	6.64
SSF	K-Tron KT20	61.70	8.20	4.16

4.2 Model testing

In this section, the model is tested over experimental data. Despite this, further experimental work is required to sufficiently determine the validity of the model for other systems.

Figures 7–8 show, respectively, the estimated feed rates of mannitol SD-100 and microcrystalline Avicel PH 102 using the K-Tron KT35, whilst in Figures 9–12 the predictions of the model when feeding several powders with the K-Tron KT20 are depicted. Figures 13–14 show the impact of operating and design variables on the effective density when a low cohesive materials such as the mannitol is fed. These results are discussed below.

4.2.1 Predictions using feeder K-Tron KT35

As can be seen in figures 7–8, the model is able to satisfactorily predict the feed rate of both powder fed with the feeder K-Tron KT35. In both cases, the prediction is relatively good despite the model was calibrated with data at significantly higher speed. A small overestimation of the mass flow rate can be observed in both simulations, with a deviation between predicted and measured time-averaged values by approximately 5%.

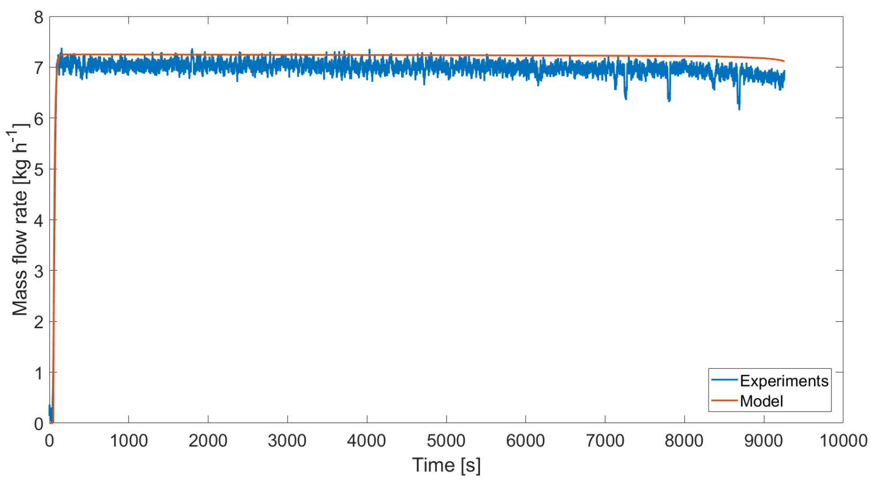

Figure 7: Predicted mass flow rate using mannitol SD-100 and feeder K-Tron KT35, screw speed 6.4 rpm. The blue line represents the measured values, the red line is the model response.

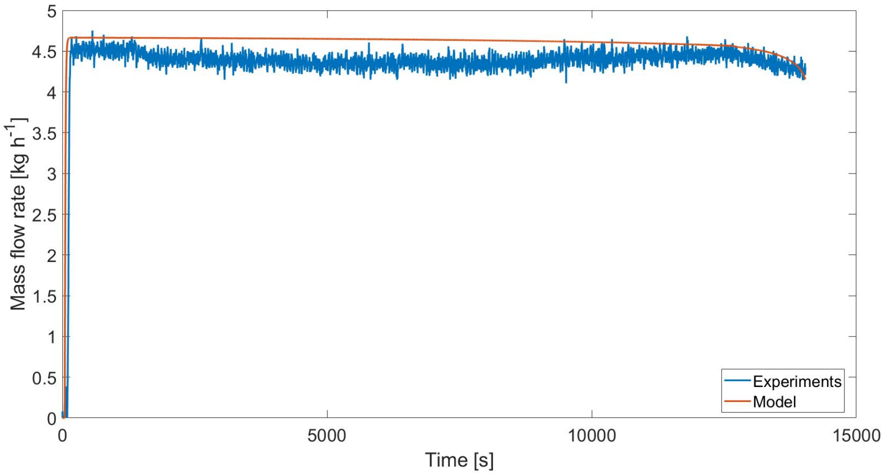

Figure 8: Predicted mass flow rate using microcrystalline cellulose Avicel PH 102 and feeder K-Tron KT35, screw speed 6.4 rpm. The blue line represents the measured values, the red line is the model response.

4.2.2 Predictions using feeder K-Tron KT20

As illustrated in Figure 9, the model can approximately estimate the feed rate after the start-up when using crosscarmellose sodium in the K-Tron KT20, despite the significant change in the operating conditions and the limited data set available for model calibration. The feed rate of crosscarmellose sodium drops at the end of the simulation because the initial hopper fill level was very low and the initial overestimation of the flow rate, due to the inaccurate dead time, causes an earlier hopper depletion. Reasonable predictions are achieved also when sodium stearate fumarate is fed, as depicted in Figure 10. Crosscarmellose sodium and sodium stearyl fumarate are two among the most cohesive powders, according to the classification based on the Hausner ratio (i.e. the ration between tapped bulk density and loose bulk density[42]), as well as the powders with the lowest values average particle size (both D_{32} and D_{43}, for further details see Table 1 in the supporting information).

For both powders, crosscarmellose sodium and sodium stearate fumarate, the initial dynamics predicted by the model is not in agreement with the experimental data. In these simulations, considering the significant different screw speeds from the ones used during the parameter estimation, the residence time has been used as estimation of the dead time. However, the experimental dead time is significantly larger. It is worth noting that both measured feed rates, at the beginning of the operation, show a first small peak approximately at the calculated residence time (at around 30 seconds for crosscarmellose sodium, Figure 9, and at around 10 seconds for sodium stearate fumarate, Figure 10). However, after the small peak, no materials is fed for a few seconds. This may be related to an irregular initial hopper discharge, perhaps caused by a powder bridge, which makes the estimation of the initial dead time particularly challenging. This phenomenon requires further investigations.

When mannitol and lactose monohydrate are fed through K-Tron KT20, the model predictions show significant discrepancies from the experimental measurements when the operating range significantly differ from calibration range (Figures 11–12). Similar results have been achieved when investigating the behaviour of microcrystalline cellulose. A larger amount of experimental data is needed for the model calibration, probably the effective density model is too simple to accurately predict the dynamics of the system for these powders in a small feeder and over a large operating range. The reason lies in the varying resistance to flow which, for the least cohesive powders such as mannitol or lactose, decreases when the screw speed significantly increases. This screw speed-dependant resistance to flow is consistent with the experimental observations reported by Freeman and Millington-Smith[57]. The variation of the effective density with significantly different screw speeds, when using mannitol with K-Tron KT20, is shown in Figure 13.

On the contrary, for crosscarmellose sodium and sodium stearyl fumarate, the effect of the screw speed on the degree of fill is limited and the model can estimate the mass flow rate over a larger operating range.

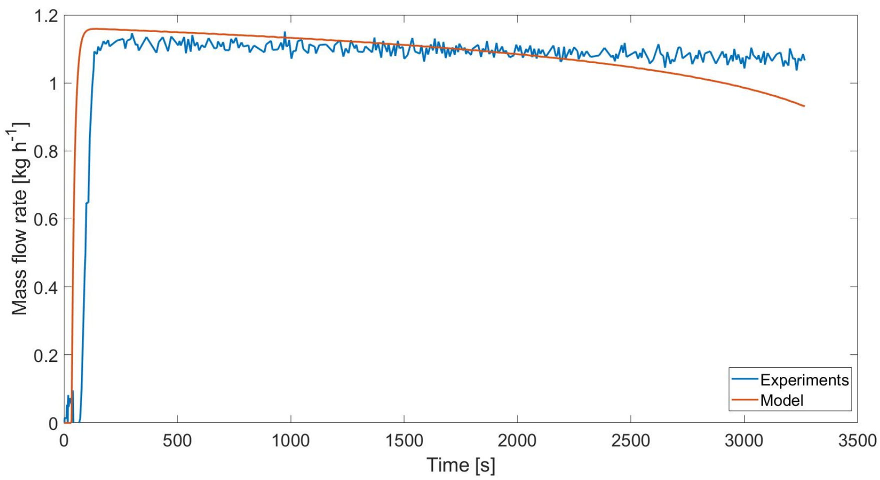

Figure 9: Predicted mass flow rate using crosscarmellose sodium and feeder K-Tron KT20, screw speed 7.71 rpm. The blue line represents the measured values, the red line is the model response.

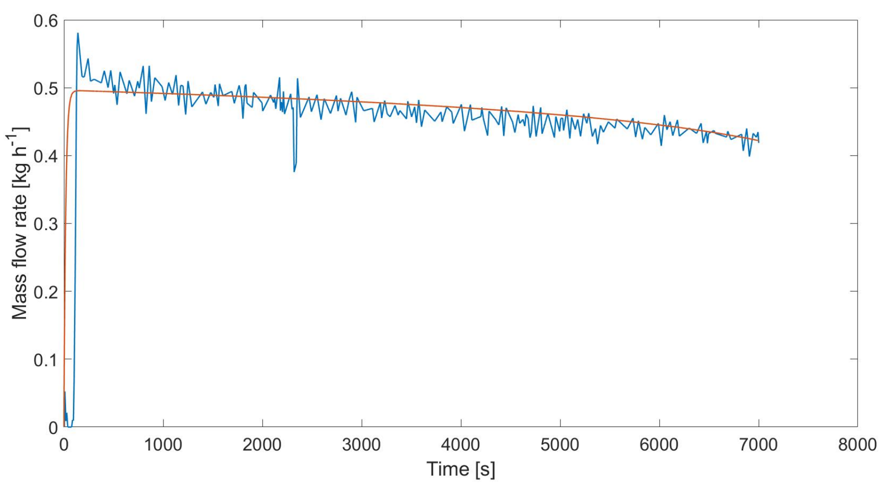

Figure 10: Predicted mass flow rate using sodium stearyl fumarate and feeder K-Tron KT20, screw speed 7.71 rpm. The blue line represents the measured values, the red line is the model response.

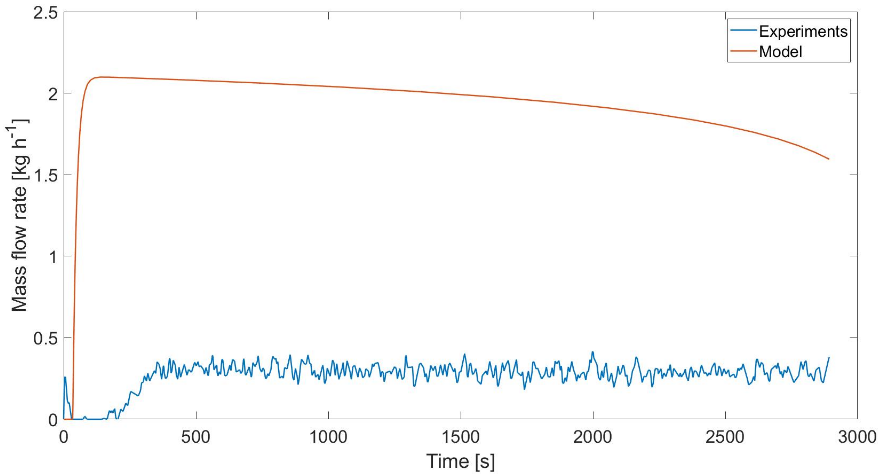

Figure 11: Predicted mass flow rate using lactose monohydrate and feeder K-Tron KT20, screw speed 7.71 rpm. The blue line represents the measured values, the red line is the model response.

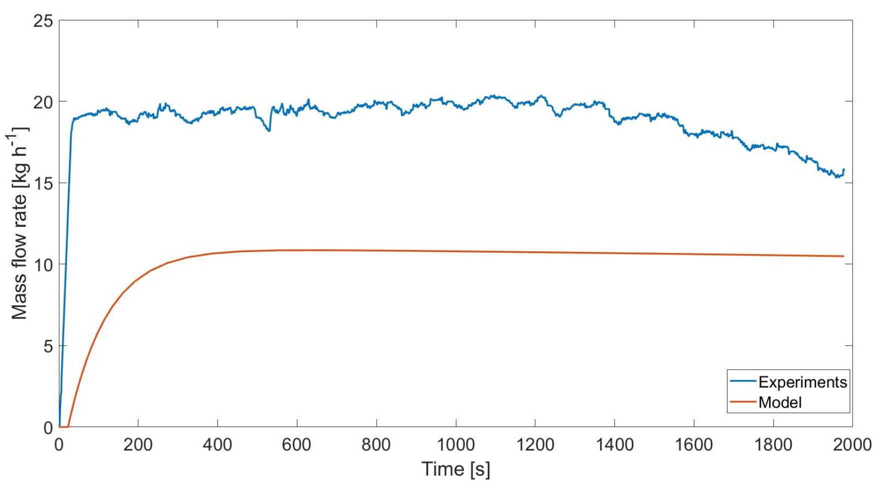

Figure 12: Predicted mass flow rate using mannitol SD-100 and feeder K-Tron KT20, screw speed 77.1 rpm. The blue line represents the measured values, the red line is the model response.

4.2.3 Impact of screw design and speed for low-cohesive powders

The screw speed-dependant resistance to flow mentioned above, for powders such as lactose monohydrate or mannitol, is intensified in small pitch volume. This can be seen in Figure 13, where mannitol is investigated in the same feeder at two significantly different screw speeds. As can be seen, for equal vertical stress, the degree of fill is significantly larger at higher screw speed. When larger screws are used (K-Tron KT35), the impact of the screw speed on the degree of fill is limited and the feeder, for similar screw speed and equal vertical stress, operates with significantly higher degree of fill (Figure 14). These results indicate that the degree of fill is a complex function of physical properties, screw speed and screw geometry and cannot be captured by shortcut models over a large operating range, in particular for low-cohesive powders and small twin screws.

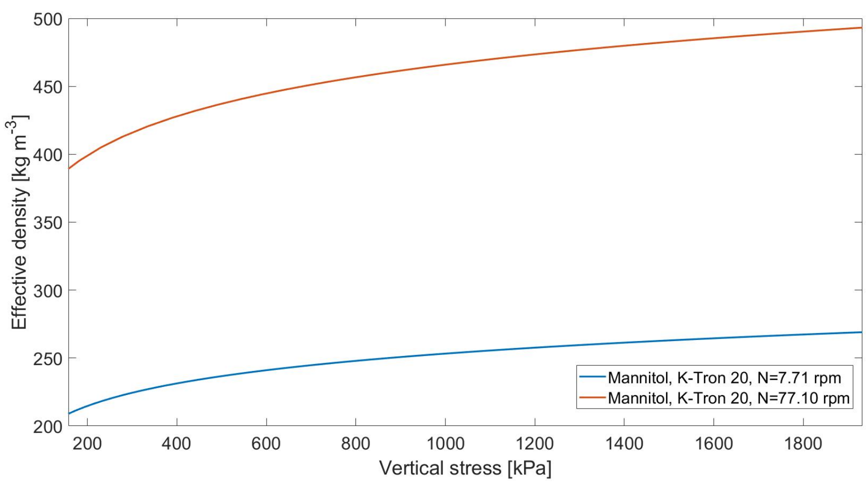

Figure 13: Effective density against vertical stress, using mannitol and K-Tron KT20 at two different screw speeds. The red line represents the simulated feed rate at 7.71 rpm, whilst the blue line represents the simulated feed rate at 77.1 rpm.

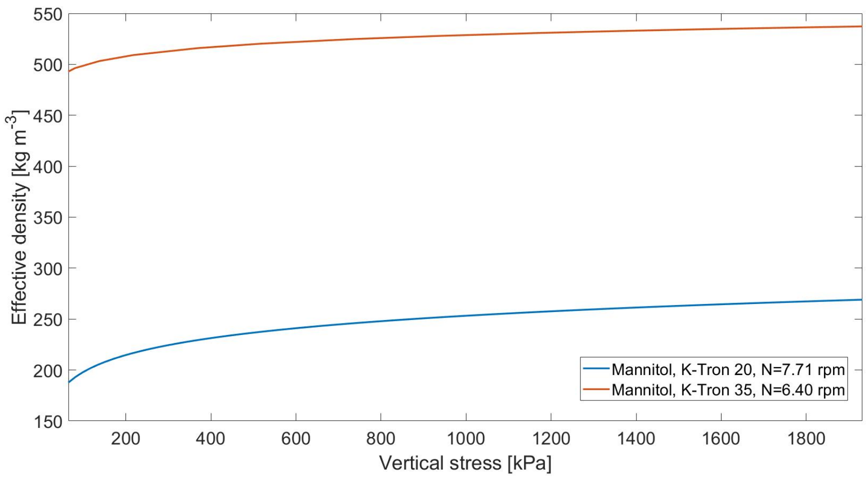

Figure 14: Effective density against vertical stress, using mannitol with both K-Tron KT20 and K-Tron KT35 at two similar screw speeds. The red line represents the simulated feed rate using K-Tron KT20, whilst the blue line represents the simulated feed rate using K-Tron KT35.

4.3 Comparison with state-of-the-art models

In this section, the performance of the model proposed in this work is compared with the models currently suggested in the literature to predict the mass flow rate out of a feeder. Three mathematical models have been used:

1. the model suggested by Boukouvala et al.[2] (Eqs. 1–2), requiring three parameters;
2. the model developed by Escotet-Espinoza[21] (Eqs. 3–4), requiring three parameters;
3. the model proposed by Yu[16] (Eq. 5), requiring one parameter.

Yu proposed a mechanistic approach to estimate the time-averaged feed rate at constant screw speed, whereas the other two models incorporates empirical relationships to predict the feed rate under gravimetric mode. The models are calibrated using experimental data of lactose monohydrate in the K-Tron KT20, at two markedly different screw speeds. For all models, significantly different parameters have been estimated. Results are compared in Figure 15 (low speed case) and Figure 16 (high speed case).

In Figure 15, the calculated feed rate using the model developed by Escotet-Espinoza et al. is not clearly visible as it is identical with the feed rate calculated by Yu's model. Apart from the model suggested in this work, the model by Boukouvala et al. is the only model able to capture the step response under volumetric mode. The model by Escotet-Espinoza et al. was developed for gravimetric mode, hence it can solely predict the step response by the increase in the screw speed during the start-up (because of the control action). Since here volumetric mode is simulated, no controller is included and no step response can be predicted, at constant screw speed, by the model suggested by Escotet-Espinoza et al.

Among the models previously suggested in the literature, the model developed by Escotet-Espinoza[21] is the only one that incorporates the effect of the hopper fill level on the feed rate. The decrease in the feed rate, as the hopper gets depleted, can be observed in Figure 16. The models developed by Yu and Boukouvala et al. do not capture this phenomena.

No models previously suggested in the literature include dead times. The model suggested in this work, as it is able to predict the initial dead time, the first order response and the slow decrease in the feed rate due to the hopper depletion, provides significantly lower deviation from the experimental measurements (in terms of mean squared error) when compared to the other models, but it requires the estimation of an additional parameter. However, when the dead time θ is replaced by the residence time, the model still provides a better agreement with experimental data, using the same number of fitting parameters as the other models. A limitation of all models is related to the necessity to recalibrate them, for certain powders, when predicting over a large operating range, due to the screw speed-dependant resistance to flow discussed in the previous sections.

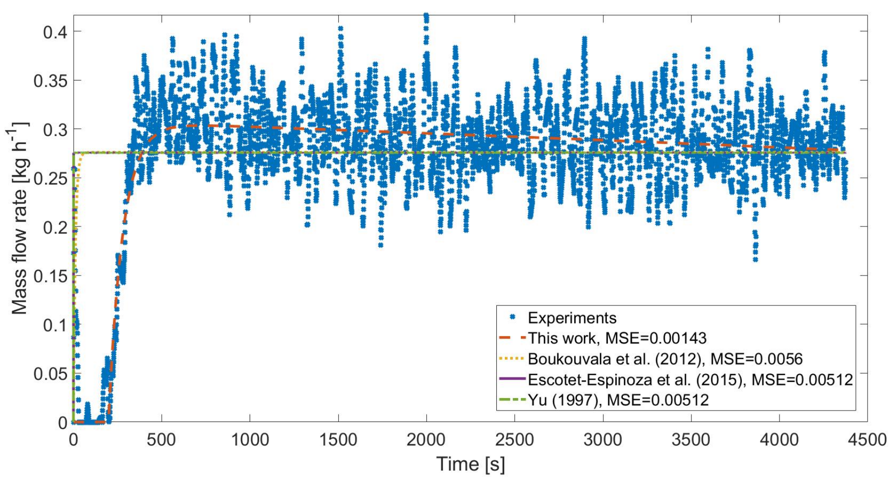

Figure 15: Comparison between mathematical models currently available in the literature. The blue dots represent experimental measurements, the continuous red line represents the calculated feed rate using the model presented in this work, the orange dotted line represents the feed rate using the model developed by Boukouvala et al., the dashed purple line represents the feed rate using the model developed by Escotet-Espinoza et al., the green dashed line represents the feed rate using the model developed by Yu. All models have been calibrated over the experimental feed rate using lactose monohydrate and feeder K-Tron KT20, at 7.71 rpm.

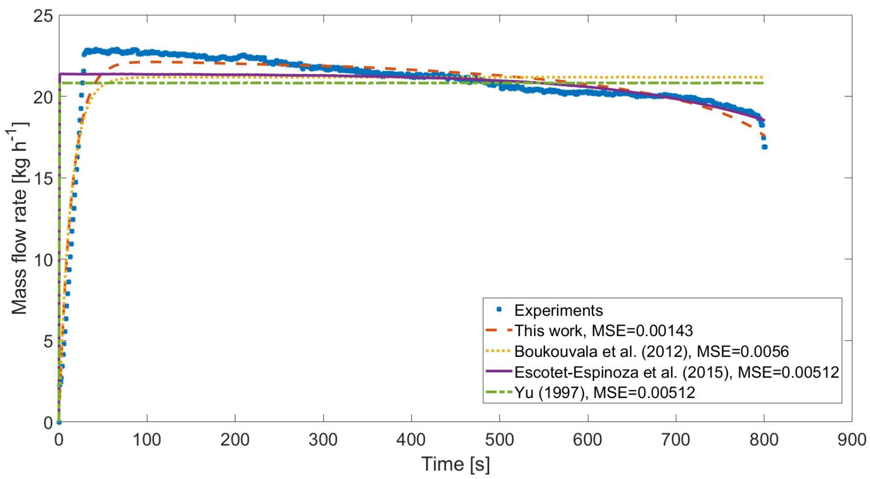

Figure 16: Comparison between mathematical models currently available in the literature. The blue dots represent experimental measurements, the continuous red line represents the calculated feed rate using the model presented in this work, the orange dotted line represents the feed rate using the model developed by Boukouvala et al., the dashed purple line represents the feed rate using the model developed by Escotet-Espinoza et al., the green dashed line represents the feed rate using the model developed by Yu. All models have been calibrated over the experimental feed rate using lactose monohydrate and feeder K-Tron KT20, at 77.1 rpm.

5 Conclusions

In this paper, a methodology for the development of a mathematical model of twin screw feeders is proposed. Hopper and screw models are combined using a hybrid mechanistic and empirical approach. A first order plus dead time model has been suggested. The model calibration has been performed for six different powders and two screw feeders. Model predictions are in good agreement with experimental values when the largest screws are used. When the small screws are employed, the model can approximately estimate the feed rates when using crosscarmellose sodium and sodium stearyl fumarate over a large operating range, although the calculation of the dead time is not accurate and requires further investigation. Mannitol SD-100, lactose monohydrate and microcrystalline cellulose Avicel PH 101 and 102 show a screw speed-dependant resistance to flow and to fill the screw pitch, particularly evident when using the small screws. This phenomenon is not captured by the model when the screw speed is investigated over a large operating range. Furthermore, the role of the agitator has not been explicitly considered in the model. These aspects requires further investigations and higher modelling complexity.

When compared to the state-of-the-art models to estimate the feed rate out of a screw feeder, the model suggested in this work provides better predictions under volumetric mode. Furthermore, the model allows to investigate the impact of friction properties (effective angle of internal friction, wall friction angle, friction coefficient) and both hopper and screws designs on the feed rate. Despite some simplifying assumptions require further investigations, the modelling approach suggested in this work represents a further step towards the development of high-fidelity mechanistic models of screw feeders.

Acknowledgement

The authors would like to acknowledge Eli Lilly and Company for funding and experimental data provided.

Supporting Information

Physical properties, further results from the model calibration and information regarding some sensitivity analyses are available at http://pubs.acs.org.

Nomenclature

Symbols	***Description***	***Units***
A	Cross sectional area	m^2
B	Parameter for stress calculation	
c	Distance between screw flight and casing	mm
D	Parameter for stress calculation	
E	Parameter for stress calculation	
ff	Feed factor	kg revolution^{-1}
g	Gravitational acceleration, 9.81	m s^{-2}
H	Height	m
k	Model parameter	
l_t	Distance between twin screw centres	m
m	Mass	kg
$\dot{m}$	Mass flow rate	kg h^{-1}
n	Number of screw starts	
N	Screw speed	rpm
P	Pitch	mm
R	Radius	mm
$\bar{S}$	Dimensionless average stress	
t	Time	s
U	Perimeter	m
z	Time delay domain (Eq. 2)	s

z	Depth	m
Z	Dimensionless depth	
V	Volume	m^3

Greek Symbols

α	Angle	$^\circ$
β	Model parameter (Eq. 3)	kg^{-1}
β	Angle (Eq. 11)	$^\circ$
phi	Angle	$^\circ$
κ	Model parameter	
μ	Friction coefficient	
η	Volumetric efficiency	
ρ	Mass density	$kg\ m^{-3}$
σ	Stress	kPa
θ	Time delay	s
Θ	Delay factor	
τ	Time constant	s
τ	Shear stress (Eq. 15)	kPa
ζ	Dimensionless length, R/P	

Subscripts and superscripts

av	Average
b	Bulk
c	Core shaft
d	Dynamic
eff	Effective
exp	Experimental
f	Fill
in	Initial

min	Minimum
o	Outer
s	Static
sat	Saturation
sw	Switch
v	Vortex (for η), vertical (for σ)

Acronysms

MSE	Mean Squared Error
MCC	Microcrystalline Cellulose
CCS	Crosscarmellose Sodium
SSF	Sodium Stearyl Fumarate

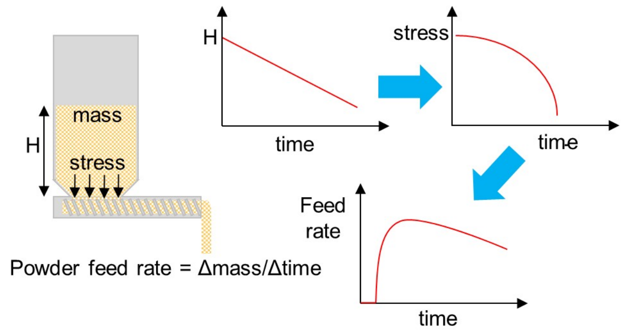

mass
H
stress
Powder feed rate = Δmass/Δtime
H
time
stress
time
Feed
rate
time

References

(1) Boukouvala, F.; Muzzio, F. J.; Ierapetritou, M. G. Design space of pharmaceutical processes using data-driven-based methods. *J Pharm Innov* **2010**, *5*, 119–137.

(2) Boukouvala, F.; Niotis, V.; Ramachandran, R.; Muzzio, F. J.; Ierapetritou, M. G. An integrated approach for dynamic flowsheet modeling and sensitivity analysis of a continuous tablet manufacturing process. *Comp & Chem Eng* **2012**, *42*, 30–47, European Symposium of Computer Aided Process Engineering - 21.

(3) Ierapetritou Marianthi,; Muzzio Fernando,; Reklaitis Gintaras, Perspectives on the continuous manufacturing of powder-based pharmaceutical processes. *AIChE J* **2016**, *62*, 1846–1862.

(4) Wang, Z.; Escotet-Espinoza, M. S.; Ierapetritou, M. Process analysis and optimization of continuous pharmaceutical manufacturing using flowsheet models. *Comp & Chem Eng* **2017**, *107*, 77–91.

(5) Wang, Y.; Li, T.; Muzzio, F. J.; Glasser, B. J. Predicting feeder performance based on material flow properties. *Powder Technol* **2017**, *308*, 135–148.

(6) Engisch, W. E.; Muzzio, F. J. Method for characterization of loss-in-weight feeder equipment. *Powder Technol* **2012**, *228*, 395–403.

(7) Engisch, W. E.; Muzzio, F. J. Feedrate deviations caused by hopper refill of loss-in-weight feeders. *Powder Technol* **2015**, *283*, 389–400.

(8) Benyahia, B.; Lakerveld, R.; Barton, P. I. A plant-wide dynamic model of a continuous pharmaceutical process. *Ind Eng Chem Res* **2012**, *51*, 15393–15412.

(9) Rogers, A. J.; Inamdar, C.; Ierapetritou, M. G. An integrated approach to simulation of pharmaceutical processes for solid drug manufacture. *Ind Eng Chem Res* **2014**, *53*, 5128–5147.

(10) Rogers, A. J.; Hashemi, A.; Ierapetritou, M. G. Modeling of particulate processes for the continuous manufacture of solid-based pharmaceutical dosage forms. *Processes* **2013**, *1*, 67–127.

(11) García-Muñoz Salvador,; Butterbaugh Adam,; Leavesley Ian,; Manley Leo Francis,; Slade David,; Bermingham Sean, A flowsheet model for the development of a continuous process for pharmaceutical tablets: An industrial perspective. *AIChE J* **2017**, *64*, 511–525.

(12) Blackshields, C. A.; Crean, A. M. Continuous powder feeding for pharmaceutical solid dosage form manufacture: a short review. *Pharma Dev Technol* **2018**, *23*, 554–560.

(13) Fonteyne, M.; Vercruysse, J.; Leersnyder, F. D.; Snick, B. V.; Vervaet, C.; Remon, J. P.; Beer, T. D. Process Analytical Technology for continuous manufacturing of solid-dosage forms. *TrAC Trends Analyt Chem* **2015**, *67*, 159 – 166.

(14) Snick, B. V.; Kumar, A.; Verstraeten, M.; Pandelaere, K.; Dhondt, J.; Pretoro, G. D.; Beer, T. D.; Vervaet, C.; Vanhoorne, V. Impact of material properties and process variables on the residence time distribution in twin screw feeding equipment. *Int J Pharma* **2019**, *556*, 200 – 216.

(15) Engisch, W. E.; Muzzio, F. J. Loss-in-weight feeding trials case study: pharmaceutical formulation. *J Pharma Innov* **2015**, *10*, 56–75.

(16) Yu, Y. Theoretical modelling and experimental investigation of the performance of screw feeders. Ph.D. thesis, University of Wollongong, 1997.

(17) Jaeger, H. M.; Nagel, S. R. Physics of the granular state. *Science* **1992**, *255*, 1523–1531.

(18) Jia, Z.; Davis, E.; Muzzio, F. J.; Ierapetritou, M. G. Predictive modeling for pharmaceutical processes using kriging and response surface. *J Pharma Innov* **2009**, *4*, 174–186.

(19) Van Snick, B.; Dhondt, J.; Pandelaere, K.; Bertels, J.; Mertens, R.; Klingeleers, D.; Di Pretoro, G.; Remon, J. P.; Vervaet, C.; De Beer, T.; Vanhoorne, V. A multivariate raw material property database to facilitate drug product development and enable in-silico design of pharmaceutical dry powder processes. *Int J Pharma* **2018**, *549*, 415–435.

(20) Bostijn, N.; Dhondt, J.; Ryckaert, A.; Szabó, E.; Dhondt, W.; Van Snick, B.; Vanhoorne, V.; Vervaet, C.; De Beer, T. A multivariate approach to predict the volumetric and gravimetric feeding behavior of a low feed rate feeder based on raw material properties. *Int J Pharma* **2019**, *557*, 342–353.

(21) Escotet-Espinoza, M. S.; Jayjock, E.; Singh, R.; et. al, Annual Meeting November 8-13. 2015.

(22) Yu, Y.; Arnold, P. C. The influence of screw feeders on bin flow patterns. *Powder Technol* **1996**, *88*, 81–87.

(23) Roberts, A. W. The influence of granular vortex motion on the volumetric performance of enclosed screw conveyors. *Powder Technol* **1999**, *104*, 56–67.

(24) Ketterhagen, W. R.; Curtis, J. S.; Wassgren, C. R.; Hancock, B. C. Predicting the flow mode from hoppers using the discrete element method. *Powder Technol* **2009**, *195*, 1–10.

(25) Imole, O. I.; Krijgsman, D.; Weinhart, T.; Magnanimo, V.; Chávez Montes, B. E.; Ramaioli, M.; Luding, S. Reprint of "Experiments and discrete element simulation of the dosing of cohesive powders in a simplified geometry". *Powder Technol* **2016**, *293*, 69–81.

(26) Rogers, A.; Ierapetritou, M. G. Discrete element reduced-order modeling of dynamic particulate systems. *AIChE J* **2014**, *60*, 3184–3194.

(27) Kretz, D.; Callau-Monje, S.; Hitschler, M.; Hien, A.; Raedle, M.; Hesser, J. Discrete element method (DEM) simulation and validation of a screw feeder system. *Powder Technol* **2016**, *287*, 131–138.

(28) Guoming, H.; Jinxin, C.; Bin, J.; Hui, W.; Liping, L. Modeling and simulation of transportation system of screw conveyors by the Discrete Element Method. 2010 International Conference on Mechanic Automation and Control Engineering. 2010; pp 927–930.

(29) Owen, P. J.; Cleary, P. W. Prediction of screw conveyor performance using the Discrete Element Method (DEM). *Powder Technol* **2009**, *193*, 274–288.

(30) Owen, P. J.; Cleary, P. W. Screw conveyor performance: comparison of discrete element modelling with laboratory experiments. *Prog Comp Fluid Dy* **2010**, *10*, 327–333.

(31) Schulze, D. *Powders and bulk solid: behavior, characterization, storage and flow*; Springer Verlag: Berlin – Heidelberg – New York, 2008.

(32) Schulze, D. The prediction of initial stresses in hoppers. *Bulk solids Handling* **1994**, *14*, 505–512.

(33) Walters, J. K. A theoretical analysis of stresses in axially-symmetric hoppers and bunkers. *Chem Eng Sci* **1973**, *28*, 779–789.

(34) Janssen, H. Versuche ueber getreidedruck in silozellen. *Z. Ver. Dtsch. Ing.* **2020**, 1045–1049.

(35) Vasilenko, A.; Koynov, S.; Glasser, B. J.; Muzzio, F. J. Role of consolidation state in the measurement of bulk density and cohesion. *Powder Technol* **2013**, *239*, 366–373.

(36) Sun, C. C. Setting the bar for powder flow properties in successful high speed tableting. *Powder Technol* **2010**, *201*, 106 – 108.

(37) Zhang, Y.; Law, Y.; Chakrabarti, S. Physical properties and compact analysis of commonly used direct compression binders. *AAPS PharmSciTech* **2003**, *4*, 489–499.

(38) Ramachandruni, H.; Hoag, S. W. Design and validation of an annular shear cell for pharmaceutical powder testing. *J Pharma Sci* **2001**, *90*, 531–540.

(39) Paul, S.; Chang, S.-Y.; Dun, J.; Sun, W.-J.; Wang, K.; Tajarobi, P.; Boissier, C.; Sun, C. C. Comparative analyses of flow and compaction properties of diverse mannitol and lactose grades. *Int J Pharma* **2018**, *546*, 39–49.

(40) Phan, H.; Banov, D.; Delancy, M.; Brockbank, K. Characterization of the properties of powder excipients commonly used in pharmaceutical compounding. *Particul Sci Technol* **2016**, *34*, 271–277.

(41) Geldart, D.; Harnby, N.; Wong, A. Fluidization of cohesive powders. *Powder Technol* **1984**, *37*, 25 – 37.

(42) Abdullah, E. C.; Geldart, D. The use of bulk density measurements as flowability indicators. *Powder Technol* **1999**, *102*, 151–165.

(43) Arnold, P.; McLean, A. Improved analytical flowfactors for mass-flow hoppers. *Powder Technol* **1976**, *15*, 279 – 281.

(44) Luyben, W. L. *Process modeling, simulation, and control for chemical engineers*, 2nd ed.; New York McGraw-Hill, 1990.

(45) Marlin, T. *Process control: designing processes and control systems for dynamic performance*; New York McGraw-Hill, 2001.

(46) Stephanopoulos, D. *Chemical process control: an introduction to theory and practice*; Prentice-Hall: New Jersey, 1984; pp 173–184.

(47) Kawakita, K.; Lüdde, K.-H. Some considerations on powder compression equations. *Powder Technol* **1971**, *4*, 61–68.

(48) Malave, J.; Barbosa-Canovas, G. V.; Peleg, M. Comparison of the compaction characteristics of selected food powders by vibration, tapping and mechanical compression. *J Food Sci* **1985**, *50*, 1473–1476.

(49) Comoglu, T. An overview of compaction equations. *J. Fac. Pharm, Ankar* **2007**, *36*, 123–133.

(50) Nordstrom, J.; Klevan, I.; Alderborn, G. A particle rearrangement index based on the Kawakita powder compression equation. *J Pharma Sci* **2009**, *98*, 1053–1063.

(51) Saw, H. Y.; Davies, C. E.; Brisson, G.; Paterson, A.; Jones, J. R. Bulk density of lactose powders under low consolidation stresses. *Conference Chemeca 2013* **2013**,

(52) Walters, J. K. A theoretical analysis of stresses in silos with vertical walls. *Chem Eng Sci* **1973**, *28*, 13–21.

(53) Jenike, A. W. *Storage and flow of solids*; Bull. No. 123, Engng. Exp. Station, Univ. of Utah: Salt Lake City (USA), 1964.

(54) Schulze, D.; Schwedes, J. An examination of initial stresses in the hoppers. *Chem Eng Sci* **1994**, *49*, 2047–2058.

(55) Strusch, J.; Schwedes, J. The use of slice element methods for calculating insert loads. *Bulk solids Handling* **1994**, *14*, 505–512.

(56) Michalowski, R. L. Approximate theory of loads in plane asymmetrical converging hoppers. *Powder Technol* **1973**, *36*, 5–11.

(57) Freeman, T.; Millington Smith, D. Predicting feeder performance from powder flow measurements. Powder Bulk Solids, 2015. Accessed 20.10.2019.